

Shaped Offset Quadrature Phase Shift Keying Based Waveform for Fifth Generation Communication

R. Ann Caroline Jenifer*, M. A. Bhagyaveni, V. Saroj Malini and M. Shanmugapriya

Department of ECE, College of Engineering Guindy, Anna University, Chennai, 600025, India

*Corresponding Author: R. Ann Caroline Jenifer. Email: anncarolinejenifer@gmail.com

Received: 28 April 2022; Accepted: 22 September 2022

Abstract: Fifth generation (5G) wireless networks must meet the needs of emerging technologies like the Internet of Things (IoT), Vehicle-to-everything (V2X), Video on Demand (VoD) services, Device to Device communication (D2D) and many other bandwidth-hungry multimedia applications that connect a huge number of devices. 5G wireless networks demand better bandwidth efficiency, high data rates, low latency, and reduced spectral leakage. To meet these requirements, a suitable 5G waveform must be designed. In this work, a waveform namely Shaped Offset Quadrature Phase Shift Keying based Orthogonal Frequency Division Multiplexing (SOQPSK-OFDM) is proposed for 5G to provide bandwidth efficiency, reduced spectral leakage, and Bit Error Rate (BER). The proposed work is evaluated using a real-time Software Defined Radio (SDR) testbed-Wireless open Access Research Platform (WARP). Experimental and simulation results show that the proposed 5G waveform exhibits better BER performance and reduced Out of Band (OOB) radiation when compared with other waveforms like Offset Quadrature Phase Shift Keying (OQPSK) and Quadrature Phase Shift Keying (QPSK) based OFDM and a 5G waveform candidate Generalized Frequency Division Multiplexing (GFDM). BER analysis shows that the proposed SOQPSK-OFDM waveform attains a Signal to Noise Ratio (SNR) gain of 7.2 dB at a BER of 10^{-3} , when compared with GFDM in a real-time indoor environment. An SNR gain of 8 and 6 dB is achieved by the proposed work for a BER of 10^{-4} when compared with QPSK-OFDM and OQPSK-OFDM signals, respectively. A significant reduction in OOB of nearly 15 dB is achieved by the proposed work SOQPSK-OFDM when compared to 16 Quadrature Amplitude Modulation (QAM) mapped OFDM.

Keywords: 5G waveform; orthogonal frequency division multiplexing; shaped offset quadrature phase shift keying; wireless open access research platform

1 Introduction

5G wireless networks envisage a huge increase in data rate, connectivity, coverage, and spectrum and energy efficiency. One of the pivotal technologies to realize the vision is to design a suitable 5G waveform. OFDM is a key enabler of fourth generation (4G) Long-Term-Evolution (LTE) because of its resilience against frequency selective fading channels, easier implementation using Fast Fourier Transform



This work is licensed under a Creative Commons Attribution 4.0 International License, which permits unrestricted use, distribution, and reproduction in any medium, provided the original work is properly cited.

(FFT), spectrum efficiency, and Multiple Input Multiple Output (MIMO) compatibility [1,2]. But it suffers from a high Peak-to-Average Power Ratio (PAPR) thereby causing signal distortion due to the non-linearity of amplifiers. OFDM also possesses large side lobes that cause interference to adjacent subcarriers. Several works of literature are found which discuss about reducing the OOB radiations. In [3], the authors propose a piecewise nonlinear companding scheme for OFDM, to attain a low PAPR. Along with PAPR, a low BER and low OOB radiation are attained. In the paper [4], the authors present a new scheme to reduce the OOB emission. The proposed system uses a new prefix/suffix OFDM precoder which makes OFDM an N-continuous system and also maintains less additive interference. In the letter [5], a new OOB reduction scheme for OFDM is presented. Short Finite Impulse Response (FIR) filters are used to reduce the complexity. The FIR filter is realized by combining a filtered cyclic prefix and complex subcarrier weighting. Several non orthogonal 5G waveforms are presented in [6] and it is seen that the non orthogonality attribute helps in alleviating strict synchronism and orthogonality requirements which are needed in many 5G applications. Universal Filtered Multicarrier (UFMC) groups subcarriers into subbands and filters them to avoid OOB radiation outside this subband [6]. In GFDM, data carried in each subcarrier is pulse shaped and transmitted [6]. This helps in reducing OOB to a greater extent. In [7], the authors present a space-time block coded (Golden Code) GFDM to achieve full diversity. BER and capacity performances are studied in a real-time scenario using the WARP SDR kit. In the letter [8], analysis of Error Vector Magnitude (EVM) based Constellation Combiner (ECC) is done in the real-time environment using the WARP kit.

SOQPSK is a continuous phase modulation technique that restricts the phase transitions to $\pm 90^\circ$, thereby reducing amplitude attenuation [9]. It employs pre modulation pulse shaping of data symbols which enables a bandwidth-efficient transmission with less spectral leakage. These characteristics of SOQPSK are advantageous for 5G scenarios. In the paper [10], an equalizer namely a maximum likelihood sequence estimator (MLSE) is proposed for aeronautical telemetry SOQPSK (SOQPSK-TG). This equalizer is based on the Ungerboeck observation model. The BER and computational complexity are evaluated under three multipath channels with increased selectivity. The BER performance of MLSE is found to be better than the minimum mean-squared error (MMSE) equalizer. A synchronization strategy and a training sequence for burst mode SOQPSK transmission are discussed in the paper [11]. An optimal training sequence is derived which jointly minimizes the Cramér–Rao bounds (CRBs) for frequency offset, phase offset, and timing offset estimation. A minimum mean squared error performance of the proposed algorithm is also presented for different versions of SOQPSK. Two digital schemes namely Pulse Code Modulation/Frequency Modulation (PCM/FM) and SOQPSK-TG are compared in [12]. BER performance and power spectrum plots are analyzed. It is seen that SOQPSK-TG has good spectral efficiency and nominal BER performance. In [13], the authors compute the capacity and pragmatic capacity of SOQPSK-TG. Also, a reduced complexity detection scheme based on Pulse Amplitude Modulation (PAM) for SOQPSK-TG is proposed. Low Density Parity Check (LDPC) codes are applied to the encoder to get a coding gain of 1.05 dB. Theoretical and practical analysis of SOQPSK-TG and Gaussian Minimum Shift Keying (GMSK) is done in [14]. The 99% bandwidth of SOQPSK-TG is reported as 3.12 MHz and as 4.4 MHz for GMSK.

In this research work, a 5G waveform namely SOQPSK based OFDM modulation is designed to provide less OOB and reduced BER. The proposed waveform is implemented and evaluated in an SDR kit namely the WARP testbed [15]. The proposed 5G waveform is compared with other modulations like OQPSK and QPSK based OFDM and GFDM.

2 System Model

2.1 SOQPSK Mapping Scheme

SOQPSK is a constant envelope, bandwidth-efficient and continuous phase modulation technique. Unlike QPSK, which has 180° and 90° phase shifts, SOQPSK restricts the carrier phase shifts to $\pm 90^\circ$.

Because of the phase restriction, the amplitude variation caused by the filtering effect of the channel is reduced. This effect is desirable since it enhances the BER performance. SOQPSK pulse shapes the complex symbols before performing modulation. This feature helps in reducing OOB radiation.

The block diagram of the SOQPSK transmitter is shown in Fig. 1 [9]. In the SOQPSK technique, the message bit stream d_i is divided into In-phase (I) and Quadrature phase (Q) channels and one of them is delayed by half symbol time ($T_s/2$) like OQPSK. The I and Q channels are sent to the precoder block [9]. The precoder generates the coefficient $\alpha_i \in \{-1, 0, 1\}$ from data d_i using the precoding algorithm which is defined in Eq. (1). The phase transition is decided as $\{-\frac{\pi}{2}, 0, +\frac{\pi}{2}\}$ based on the value of α_i . α_i never assumes the value of $\{1, -1\}$ for the consecutive bits and vice versa [9].

$$\alpha_i = \frac{(-1)^{i+1} d_{i-1} (d_i - d_{i-2})}{2} \tag{1}$$

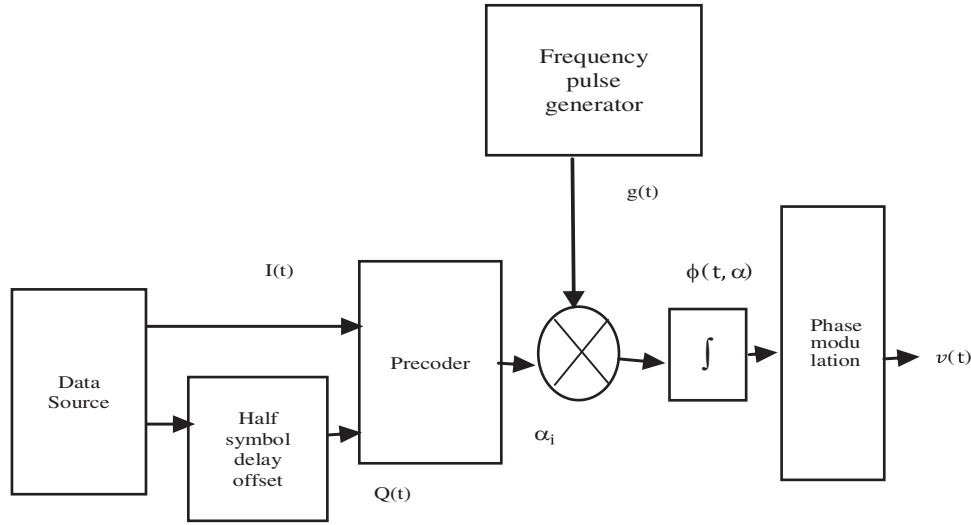


Figure 1: Block diagram of SOQPSK modulator

The precoder output is pulse shaped by the frequency pulse $g(t)$ [16] whose equation is given in Eq. (2). The function $n(t)$ is the raised cosine impulse [16] and $w(t)$ [16] is the window function whose equations are defined in Eqs. (3) and (4) respectively.

$$g(t) = n(t)w(t) \tag{2}$$

$$n(t) = \frac{A \cos((\pi \rho B t) / T_s) \sin(\frac{\pi B t}{T_s})}{1 - 4(\frac{\rho B t}{T_s})^2 \frac{(\frac{\pi B t}{T_s})}{(\frac{\pi B t}{T_s})}} \tag{3}$$

$$w(t) = \begin{cases} 1 & \text{for } \left| \frac{t}{T_s} \right| < T_1 \\ \frac{1}{2} + \frac{1}{2} \cos\left(\frac{\pi \left| \frac{t}{T_s} \right| - T_1}{T_2}\right) & \text{for } T_1 < \left| \frac{t}{T_s} \right| < T_1 + T_2 \\ 0 & \text{for } T_1 < \left| \frac{t}{T_s} \right| < T_2 \end{cases} \tag{4}$$

The phase φ of the SOQPSK signal is given in Eq. (5) [10,17]. It is continuously varied according to $g(t)$. Here m is the modulation index and its value is taken as $m = 1/2$.

$$\varphi(t, \alpha) = 2\pi m \sum_{-\infty}^{\infty} \alpha_i g(t - iT_s) dt \quad (5)$$

The complex SOQPSK signal is represented as in Eq. (6),

$$v(t, \alpha) = \sqrt{\frac{E_S}{T_S}} e^{j\varphi(t, \alpha)} \quad (6)$$

where T_S is the symbol interval and E_S is the energy per symbol, $\alpha = \{\alpha_i\}$ is the transmitted symbol sequence drawn from the ternary alphabet $\alpha_i \in \{-1, 0, 1\}$.

2.2 Proposed Work: SOQPSK Based OFDM Modulation

In this section, the design equations of the proposed work-SOQPSK based OFDM modulation are presented. The block diagram of the proposed work is shown in Fig. 2. The binary data sequence d_i is given as input to the SOQPSK modulation block. The incoming bits are divided into In-phase and Quadrature Phase streams and the Q stream is offset by half symbol time. The I and Q streams pass through the precoder to generate the coefficient $\alpha_i \in \{-1, 0, 1\}$ which is pulse shaped according to Eq. (5). The SOQPSK signal is then generated whose equation is given in Eq. (6). The SOQPSK mapped symbols V are sent to the OFDM modulator, where the Serial-to-Parallel converter converts the serial stream of SOQPSK symbols into a parallel stream which has a set of N parallel SOQPSK symbols $V_k, k = 0, 1, \dots, N-1$ corresponding to N subcarriers. Then the IFFT block converts the frequency samples into time domain samples which are given as $x_k, k = 0, 1, \dots, N-1$ and then the cyclic prefix is added. This is followed by Parallel-to-Serial conversion and Digital to Analog Conversion (DAC). The SOQPSK mapped OFDM signal is represented as in Eq. (7).

$$x(t) = \frac{1}{\sqrt{N}} \sum_{k=0}^{N-1} V_k e^{j2\pi kt/NT_N}, 0 \leq t < NT_N \quad (7)$$

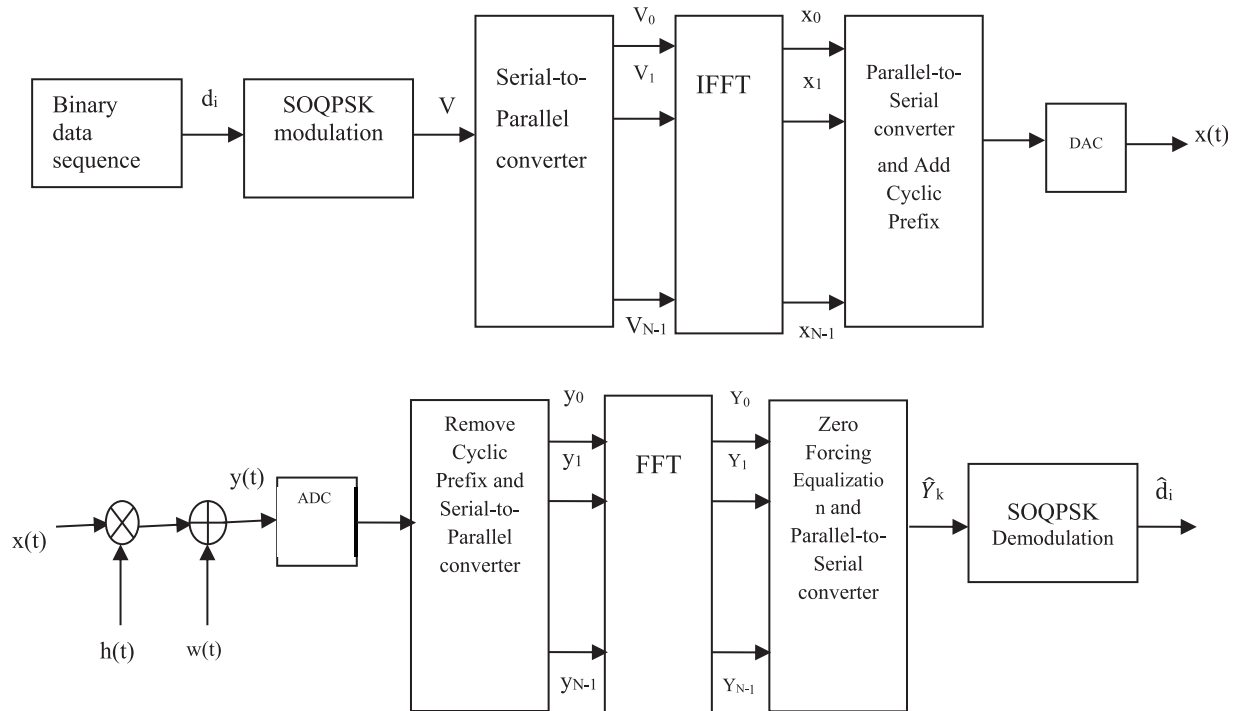


Figure 2: Proposed 5G waveform: SOQPSK based OFDM modulation

In Eq. (7), x_0, x_1, \dots, x_{N-1} represent N samples of $x(t)$ sampled at every $\frac{1}{NT_N}$ seconds. The length of the cyclic prefix is η samples and the total length of the signal $x(t)$ is $N + \eta$ samples. The signal at the receiver is given as in Eq. (8),

$$y(t) = x(t) * h(t) + w(t) \quad (8)$$

where, $h(t)$ is the channel impulse response and $w(t)$ is the Additive White Gaussian Noise (AWGN) with zero mean and variance σ^2 , $w \sim \mathcal{N}(0, \sigma^2)$. At the receiver, the cyclic prefix is removed and the samples undergo Serial-to-Parallel conversion. The parallel streams of samples y_k are sent to the FFT block. The output of the FFT block is given as in Eq. (9),

$$Y_k = X_k H_k + W_k \quad (9)$$

In Eq. (9), H_k is the FFT of the samples of the channel $h(t)$ given as h_0, \dots, h_η . Here, Zero Forcing (ZF) channel equalization (frequency equalization) is done to remove the effects of the channel. The equation for channel equalization is given in Eq. (10).

$$\hat{Y}_k = H_k^{-1} Y_k = H_k^{-1} X_k H_k + H_k^{-1} W_k = X_k + \hat{W}_k \quad (10)$$

Now, the equalized samples \hat{Y}_k are passed through the SOQPSK demodulation block. The correlation receiver performs demodulation to yield the estimate of the transmitted binary sequence \hat{d}_i as shown in Eq. (11).

$$\hat{d}_i = \int_0^{T_s} \hat{y}(t) e^{-j\varphi(t, \alpha)} dt = \int_0^{T_s} \{x(t) + \hat{w}(t)\} e^{-j\varphi(t, \alpha)} dt$$

$$\hat{d}_i = \pm \sqrt{E_S} + \hat{w} \quad (11)$$

3 Experimental Setup

3.1 WARP Radio Board

WARP version 3 (v3) radio board is a programmable and scalable SDR developed at Rice University [18]. It facilitates the designing, prototyping and testing of various physical and network layer protocols of wireless networks. The hardware feature consists of Xilinx Virtex-6 LX240T Field Programmable Gate Array (FPGA) processor, 2 programmable Radio Frequency (RF) transceivers with a frequency of operation 2.4/5 GHz and a RF bandwidth of 40 MHz. WARP SDR uses an FMC-RF-2X 245 (FPGA Mezzanine Connector) module as an expansion slot to attach 2 more RF antennas. This helps in creating a 2×2 MIMO scenario. The WARP board also consists of a 12-bit 170MSps Digital to Analog Converter (DAC), 12-bit 100MSps Analog to Digital Converter (ADC) and Dual-band 20dBm Power Amplifier (PA) [15].

The WARPLab and OFDM Reference Design allow the users to design and customize the OFDM Physical layer (PHY) and also provide an interface between the host system and the radio board. The software part uses MATLAB for signal processing [15].

3.2 Experimental Setup and Implementation of the Proposed Work

To evaluate the performance of the proposed work, we designed and implemented the SOQPSK-OFDM waveform in the WARP v3 SDR kit. The experimental set up consisted of one Personal Computer (PC), one WARP v3 radio board, 2 RF transceivers and peripherals like power cable, Ethernet cable and Joint Test Action Group (JTAG) programming cable to configure the FPGA. A Single Input Single Output (SISO) system (1 transmitter and 1 receiver) was established. The distance between the transmitting antenna and

receiving antenna was set to 30 cm. The set-up was placed in an indoor laboratory environment. The real-time channel was taken as a Rician flat fading channel for an indoor environment.

The experimental set-up and the flow diagram of SOQPSK-OFDM implementation in the WARP testbed are shown in Figs. 3. and 4. respectively. From Fig. 4, we can see that the WARPLab Reference design is used to design the SOQPSK modulator, to set the OFDM parameters, to generate preambles and payload, and to implement the OFDM block etc. WARPLab Reference design is implemented using MATLAB software. The baseband signal of the SOQPSK-OFDM waveform is thus generated. It is dumped into the FPGA board, wherein DAC conversion takes place followed by the generation of RF signal. The RF signal is transmitted via the transmitting antenna and it is passed through the channel. The receiver antenna receives the signal and sends it through a Low Noise Amplifier (LNA) and ADC. The received signal samples are sent to the WARPLab for channel equalization and demodulation processes. The channel is estimated at the receiver using preamble, Short Training Sequence (STS) and Long Training Sequence (LTS) [18]. After demodulation, the calculation of BER is done.

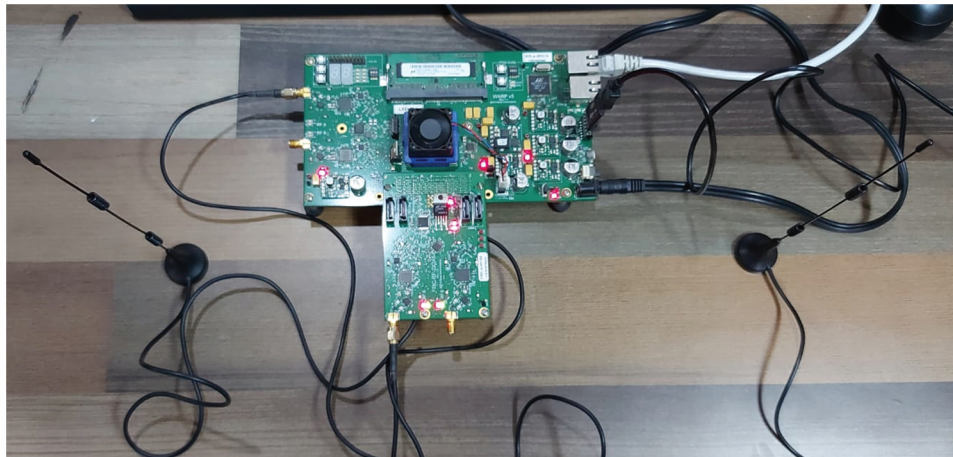


Figure 3: WARP testbed

4 Results and Discussion

In this section, we present the evaluation procedure and performance analysis of the proposed 5G waveform, SOQPSK based OFDM modulation. The system parameters are given in Table 1.

The parameters ρ , B , T_1 , T_2 , and A determine the frequency of the pulse shaping impulse and window function, whose values are taken from [9]. The number of subcarriers for OFDM modulation is taken as $N = 64$, out of which 48 are assigned as data subcarriers and 4 as pilot subcarriers. The cyclic prefix length is fixed as 16. The total number of data symbols generated is 48000.

The I and Q waveforms of the transmitted and received signals are shown in Figs. 5a and 5b. The received constellation of the SOQPSK-OFDM waveform after passing through a real-time channel is shown in Fig. 6a. Fig. 6b. shows the received constellation of QPSK-OFDM. It is observed from the results that the constellation of the proposed work shows lesser amplitude distortions because of the pulse shaping effect.

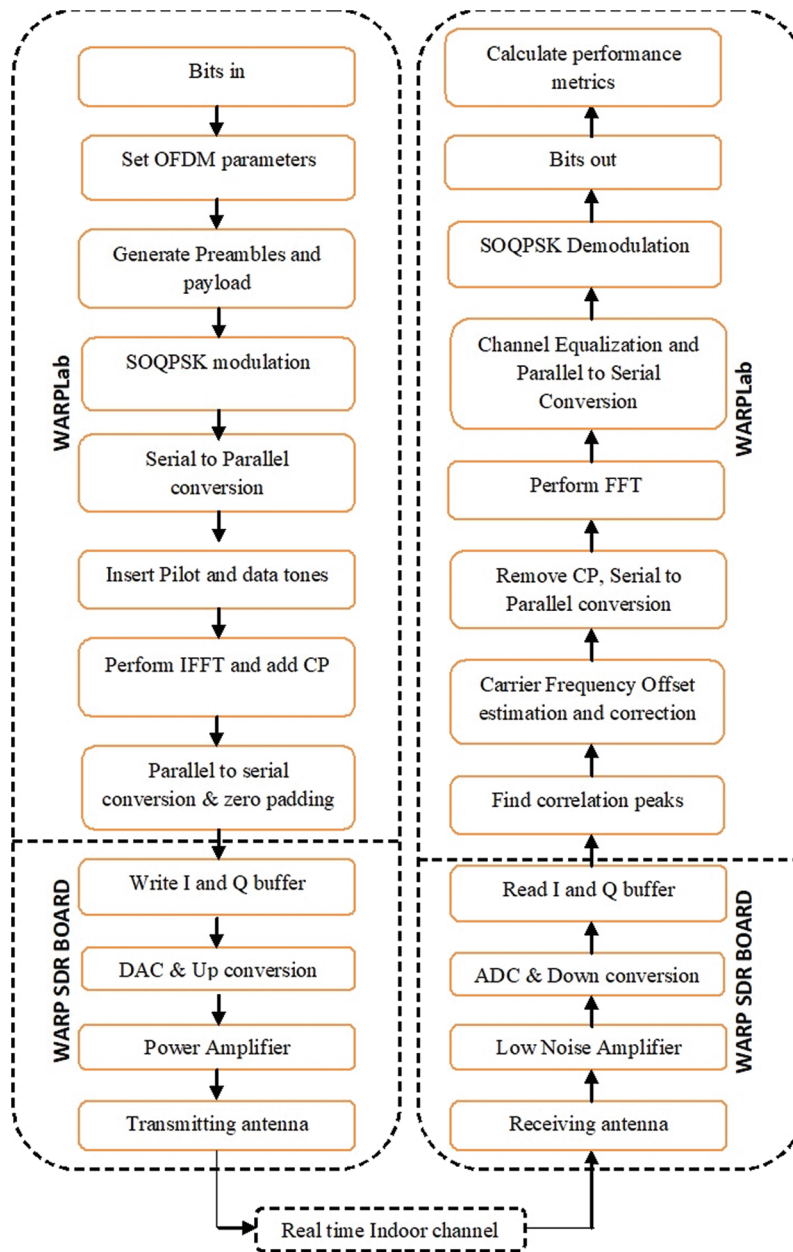


Figure 4: Flow diagram of the implementation of SOQPSK-OFDM in WARP testbed

Table 1: Simulation parameters (Values of ρ, B, T_1, T_2, A are taken from [9])

Symbol	Description	Value
ρ	Roll-off factor	0.7
B	Time scaling factor	1.25
T_1	Pulse duration	1.5
T_2	Pulse duration	0.5
A	Scaling factor to normalize the pulse shape	5399.2
N	No. of subcarriers	64
	No. of data subcarriers	48

(Continued)

Table 1 (continued)

Symbol	Description	Value
η	No. of pilot subcarriers	4
	Cyclic prefix length	16
	No. of data symbols	48000
	No. of transmit antennas	1
	No. of receive antennas	1
	Channel bandwidth	20 MHz
	Channel equalization	Zero forcing
	Mapping	SOQPSK/OQPSK/QPSK

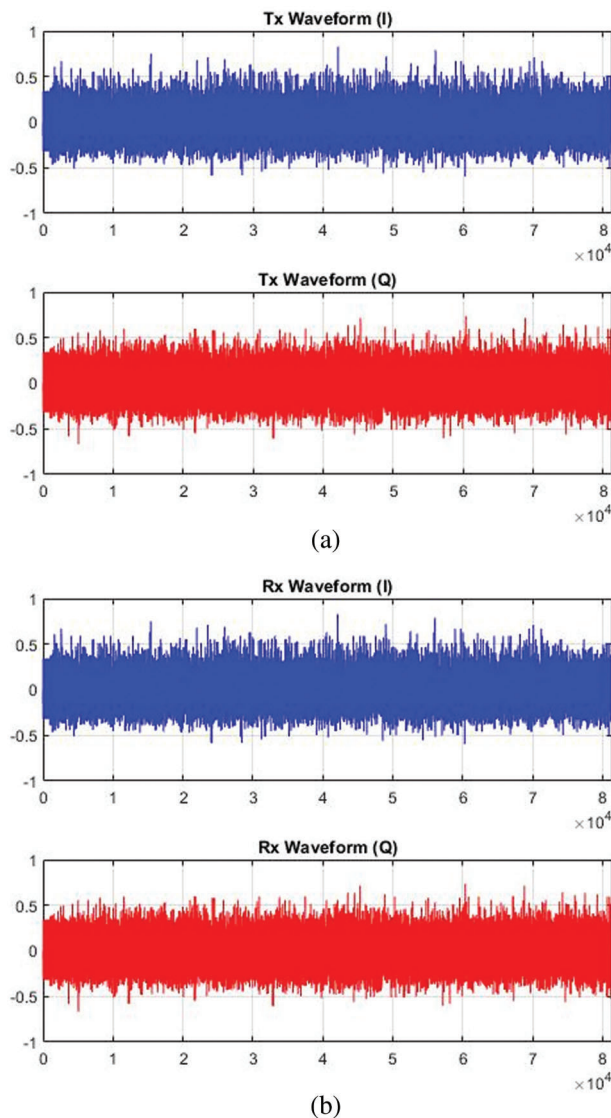


Figure 5: (a) I and Q channels of real-time transmitted SOQPSK-OFDM signal in WARP testbed; (b) I and Q channels of real-time received SOQPSK-OFDM signal in WARP testbed

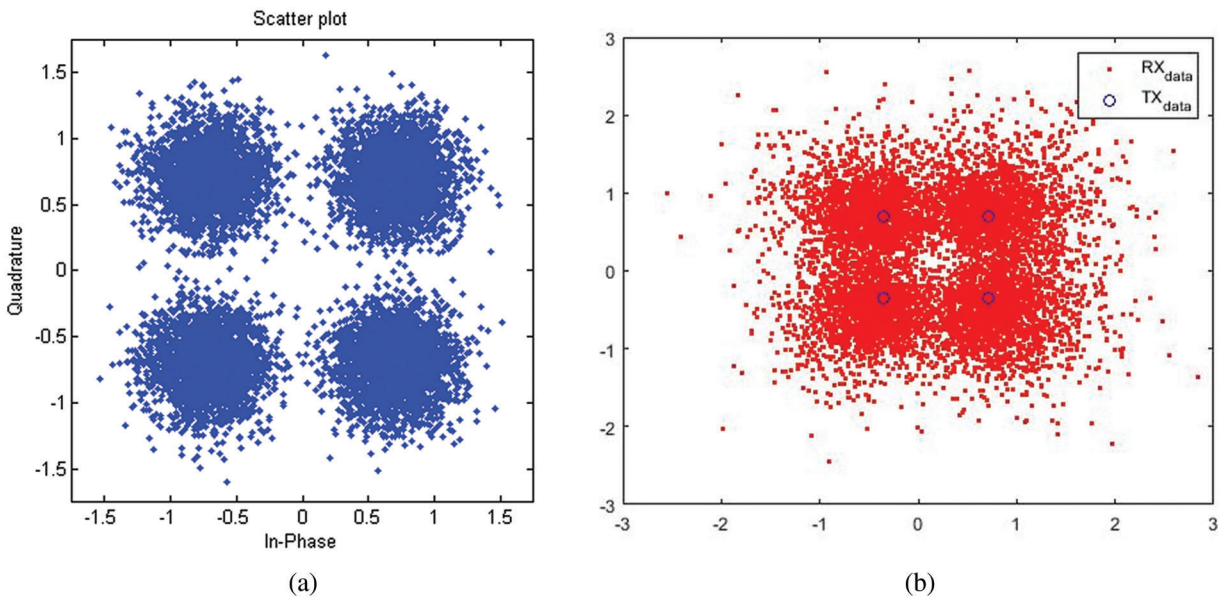


Figure 6: (a) The received signal constellation of SOQPSK-OFDM signal and (b) QPSK-OFDM signal in a WARP set-up

The BER performance of the proposed 5G waveform SOQPSK based OFDM modulation is analyzed in an indoor real-time environment using the WARP testbed. The BER vs. SNR plot of SOQPSK-OFDM is presented in Fig. 7. The proposed work is compared with other mapping techniques such as QPSK-OFDM, OQPSK based OFDM and GFDM. From Fig. 7 we can see that in order to achieve a BER of 10^{-4} , SOQPSK-OFDM needs an SNR of 28.3 dB whereas the other mapping schemes OQPSK and QPSK need an SNR of 34.3 and 36.3 dB respectively. From the results, we can infer that a better BER performance is achieved for SOQPSK based OFDM modulation. The gain in SNR is about 8 dB and 6 dB for a BER of 10^{-4} when compared with QPSK and OQPSK schemes respectively. An SNR gain of 7.2 dB is achieved for a BER of 10^{-3} by the proposed 5G waveform when compared with GFDM. The SNR gain and improvement in BER performance of SOQPSK-OFDM is because of the confined phase transition $\pm 90^\circ$ that enables lesser amplitude fluctuations in the signal.

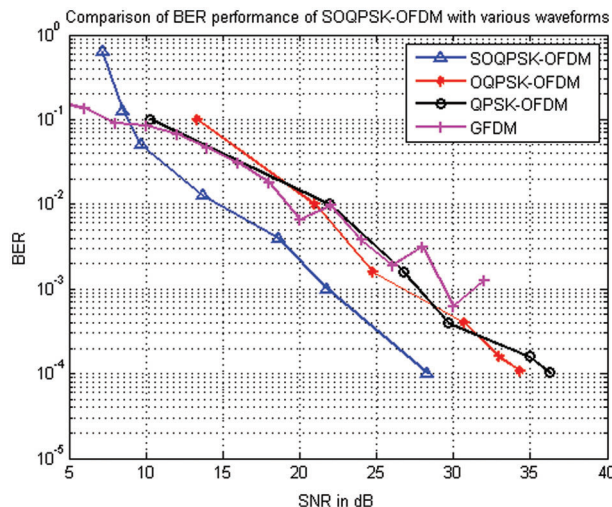


Figure 7: BER vs. SNR plot of the SOQPSK-OFDM (proposed), OQPSK-OFDM, QPSK-OFDM, and GFDM waveforms implemented in WARP testbed

The next analysis is based on the variants of SOQPSK waveforms. Table 2 shows different values of SOQPSK parameters [19]. Fig. 8 shows the BER performance of the variants of SOQPSK modulation. From Fig. 8 we can see that in order to achieve a BER of 10^{-5} , an SNR of 12 dB is needed for the SOQPSK variant considered in this work, whereas, SOQPSK-A, SOQPSK-B and SOQPSK-C need 13, 11 and 10.5 dB respectively. The difference in SNR gain is because of the different pulse shapes.

Table 2: SOQPSK parameters (values taken from [19])

Variants of SOQPSK	ρ	B	T_1	T_2
SOQPSK-A	1.0	1.35	1.4	0.6
SOQPSK-B	0.5	1.45	2.8	1.2
SOQPSK-C	0.2	2.05	1.8	0.2
SOQPSK-this work	0.7	1.25	1.5	0.5

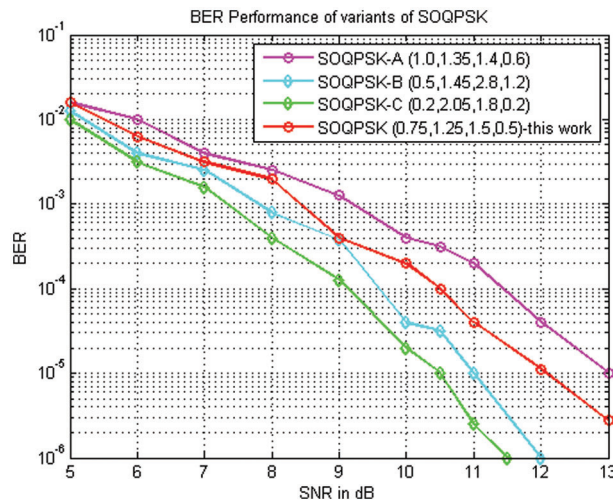


Figure 8: BER curves of variants of SOQPSK

Fig. 9 shows the power spectral density plots of the proposed 5G waveform SOQPSK-OFDM and other waveforms like Binary Phase Shift Keying (BPSK)/QPSK/16 QAM-OFDM. The evaluation result shows a significant reduction in the sideband power of the proposed work when compared to the other schemes. From the results, we can note that SOQPSK-OFDM achieves a 15 dB reduction in sideband power when compared with 16 QAM-OFDM. This is greatly advantageous.

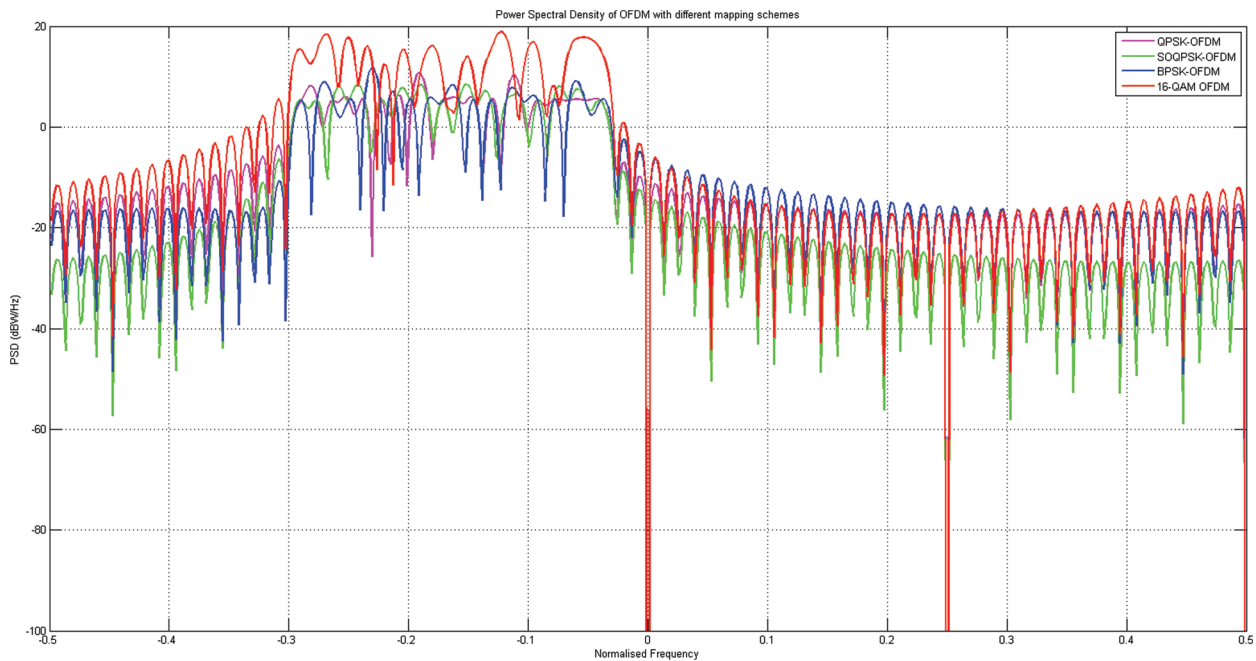


Figure 9: Performance comparison of Power spectral density of BPSK/QPSK/SOQPSK (proposed)/16 QAM-OFDM

5 Conclusion

An SOQPSK based OFDM modulation for 5G communication is proposed in this work to attain a better BER performance and reduced spectral re-growth. A novel waveform for 5G is designed by combining the SOQPSK modulation scheme with a 4G multicarrier waveform OFDM. The new waveform is proposed to overcome the disadvantages of OFDM such as high OOB and signal distortions caused by the nonlinearity in high power amplifiers at the receiver. To analyze the performance of the designed novel 5G waveform, we have conducted WARP SDR based experiments in a real-time indoor environment. Other 4G and 5G based waveforms like QPSK/OQPSK-OFDM and GFDM respectively are also implemented in the WARP testbed for comparison purposes. The experimental results indicate that the proposed SOQPSK-OFDM waveform shows better performance in terms of BER and OOB radiation when compared to the other waveforms. BER performance shows that the proposed work achieves an SNR gain of 8 and 6 dB at a BER of 10^{-4} when compared with OQPSK-OFDM and QPSK based OFDM waveforms respectively. When comparing SOQPSK-OFDM with a 5G waveform GFDM, an SNR gain of 7.2 dB is achieved by the proposed waveform for a BER of 10^{-3} . The power spectrum density analysis of SOQPSK-OFDM shows an excellent reduction in side lobes which enhances its spectral containment. An OOB reduction of nearly 15 dB is achieved by the proposed work when compared to the 16 QAM mapped OFDM waveform. The BER improvement, SNR gains and OOB reduction make SOQPSK-OFDM a suitable candidate for 5G. As part of our future work, we will extend our design to Non Orthogonal Multiple Access (NOMA) technique and test its feasibility using the SDR kit.

Authorship Contribution Statement: The authors confirm contribution to the paper as follows: study conception and design: R. Ann Caroline Jenifer, Dr. M. A. Bhagyaveni, V. Saroj Malini and Dr. M. Shanmugapriya; data collection: R. Ann Caroline Jenifer, Dr. M. A. Bhagyaveni, V. Saroj Malini and Dr. M. Shanmugapriya; analysis and interpretation of results: R. Ann Caroline Jenifer, Dr. M. A. Bhagyaveni, V. Saroj Malini and Dr. M. Shanmugapriya; draft manuscript preparation: R. Ann Caroline

Jenifer, Dr. M. A. Bhagyaveni, V. Saroj Malini and Dr. M. Shanmugapriya. All authors reviewed the results and approved the final version of the manuscript.

Funding Statement: The authors received no specific funding for this study.

Conflicts of Interest: The authors declare that they have no conflicts of interest to report regarding the present study.

References

- [1] T. Hwang, C. Yang, G. Wu, S. Li and G. Y. Li, "OFDM and its wireless applications: A survey," *IEEE Transactions on Vehicular Technology*, vol. 58, no. 4, pp. 1673–1694, 2009.
- [2] Draft Standard for Broadband over Power Line Networks: Medium Access Control and Physical Layer Specifications, IEEE Unapproved Draft Std P1901/D2.01, 2010. [Online]. Available: <https://ieeexplore.ieee.org/document/5385162>.
- [3] Z. Xing, K. Liu, B. Tang and Y. Liu, "Novel PAPR reduction scheme based on piecewise nonlinear companding transform in OFDM systems," *IEEE Communications Letters*, vol. 24, no. 8, pp. 1751–1761, 2020.
- [4] T. Taheri, R. Nilsson and J. Beek, "Quasi-cyclic symbol extensions for shaping the OFDM spectrum," *IEEE Transactions on Wireless Communications*, vol. 17, no. 10, pp. 7054–7066, 2018.
- [5] R. A. Pitaval and B. M. Popović, "Filtered-prefix OFDM," *IEEE Communications Letters*, vol. 23, no. 1, pp. 28–31, 2019.
- [6] I. S. Gaspar, N. Michailow and L. L. Mendes, "5G waveform candidate selection D3.2. version 1.3," 2015. [Online]. Available: https://www.is-wireless.com/wp-content/uploads/2015/07/5GNOW_Deliverables-5G-Waveform-Candidate-Selection-part-2.pdf.
- [7] A. C. J. Rajappa, S. D. Ramadhas, B. M. Anjaneyulu and M. R. Kuppusamy, "Golden coded GFDM for 5G communication," *Wireless Personal Communication*, vol. 115, no. 3, pp. 2335–2348, 2020.
- [8] M. R. Kuppusamy, S. M. Bokhari and B. M. Anjaneyalu, "Error vector magnitude (EVM)-based constellation combiner for cooperative relay network," *IEEE Communications Letters*, vol. 20, no. 2, pp. 304–307, 2016.
- [9] T. Hill, "An enhanced, constant envelope, interoperable shaped offset QPSK (SOQPSK) waveform for improved spectral efficiency," in *Proc. of the Int. Telemetry Conf.*, San Diego, CA, 2000.
- [10] M. Rice and E. Gagakuma, "Approximate MLSE equalization of SOQPSK-TG in aeronautical telemetry," *IEEE Transactions on Aerospace and Electronic Systems*, vol. 55, no. 2, pp. 769–784, 2019.
- [11] E. Hosseini and E. Perrins, "Burst-mode synchronization for SOQPSK," *IEEE Transactions on Aerospace and Electronic Systems*, vol. 55, no. 6, pp. 2707–2718, 2019.
- [12] B. Umashankar, S. Aswathy, N. N. S. S. R. K. Prasad, C. Bhattacharya and K. K. Naik, "SOQPSK – A spectrally efficient modulation scheme for aeronautical telemetry applications," in *Proc. IJESIT*, India, vol. 2, no. 2, pp. 383–388, 2013.
- [13] C. Sahin and E. Perrins, "The capacity of SOQPSK-TG," in *Proc. MILCOM 2011*, Baltimore, Maryland, USA, pp. 555–560, 2011.
- [14] U. Balasubramanian, P. R. Pacharne, P. Radhakrishna, K. K. Naik and C. Bhattacharya, "Telemetry applications of SOQPSK and GMSK based modulation for airborne platforms," in *Proc. CODIS*, Kolkata, India, pp. 17–20, 2012.
- [15] WARP project-Wireless open Access Research Platform WARP Radio board overview, 2022. [Online]. Available: <http://warpproject.org> (accessed on: March).
- [16] T. Nelson, E. Perrins and M. Rice, "Near optimal common detection techniques for shaped offset QPSK and Feher's QPSK," *IEEE Transactions on Communications*, vol. 56, no. 5, pp. 724–735, 2008.
- [17] T. J. Hill, "A non-proprietary, constant envelope, variant of shaped offset QPSK (SOQPSK) for improved spectral containment and detection efficiency," in *Proc. MILCOM, 2000 21st Century Military Communications Architectures and Technologies for Information Superiority*, Los Angeles, California, vol. 1, pp. 347–352, 2000.
- [18] P. Murphy, A. Sabharwal and B. Aazhang, "Design of WARP: A wireless open-access research platform," in *Proc. 14th European Signal Processing Conf.*, Florence, Italy, pp. 1–5, 2006.
- [19] M. Geoghegan, "Optimal linear detection of SOQPSK," in *Proc. Int. Telemetry Conf.*, San Diego, California, 2002.